Journal of Nano- and Electronic Physics
Vol. 8 No 3, 03045(5pp) (2016)

Журнал нано- та електронної фізики
Том 8 № 3, 03045(5cc) (2016)

Multilayer Nitride Coatings (TiZrNbHf)N/MoN

D.A. Kolesnikov[1], U.S. Nyemchenko[2], V.M. Beresnev[2], O.V. Sobol'[3], V.A. Novikov[1], S.V. Lytovchenko[2], V.A. Stolbovoi[4], I.Yu. Goncharov[1], P.V. Turbin[5], L.V. Malikov[5]

[1] *Belgorod State National Research University, 85, Peremohy St., 308015 Belgorod, Russia*
[2] *V.N. Karazin Kharkiv National University, 4, Svobody sq., 61022 Kharkiv, Ukraine*
[3] *National Technical University "Kharkiv Polytechnic Institute", 21, Kyrpychova St., 61002 Kharkiv, Ukraine*
[4] *National Science Center "Kharkiv Institute of Physics and Technology", 1, Akademichna St., 61108 Kharkiv, Ukraine*
[5] *Science Center of Physics and Technology of MES and NAS of Ukraine, 6, Svobody sq., 61022 Kharkiv, Ukraine*

(Received 28 May 2016; published online 03 October 2016)

It is shown that at low negative bias potential applied to the substrate during the deposition (U_b is less than 150 V), a two-phase state with the preferred orientation of crystallites can be reached for the multilayer coatings with the layer thickness of 50 nm. This causes high hardness (up to 59 GPa) and high adhesion strength at the same time (critical load reaches 124.9 N). Low wear resistance of the coatings in contact with the counterbody of Al_2O_3 is observed.

Keywords: Vacuum-arc deposition, High entropy alloys, Multilayer nitride coatings, Physical and mechanical properties of coatings.

DOI: 10.21272/jnep.8(3).03045 PACS numbers: 61.46. – w, 62.20.Qp, 62-65. – g

1. INTRODUCTION

Recently, considerable attention has been paid to the development and study of multilayer protective coatings with more advanced mechanical properties (in particular, high hardness) and increased thermal stability. These coatings are formed by the structural self-organization of materials [1, 2].

The perfection of properties of the mentioned compositions can be achieved by forming coatings in the nanoregion with a certain architecture of construction [3, 4]. The design of a multilayer coating, i.e. the total thickness and the thickness of nanolayers, has an effect on its mechanical properties [5]. The behavior of multilayer coatings with different layer thickness is very important in high-temperature tests.

In this regard, the concept of creating nitride and carbide coatings based on high entropy (or, in some works, multi-element) systems (HES) is being actively developed [6-9]. The coatings produced based on HES of strong nitride-forming elements, such as titanium, niobium, zirconium, hafnium, occupy a special place among the HES exhibiting the highest functional characteristics.

Thus, the use of high entropy alloys as nitride layers creates prerequisites for the thermal stability of the product material that is caused by the process of element-structural ordering in high entropy multi-element alloys with increasing temperature [10, 11].

This work is devoted to the study of the mechanical characteristics of multilayer coatings. Coatings based on nitrides of multi-element alloy (Ti-Zr-Nb-Hf) and transition VI group metal Mo were used as layers.

2. EXPERIMENTAL

A cathode of the following composition was produced for the deposition of multilayer coatings: Ti – 30 wt. %; Zr – 30 wt. %; Nb – 25 wt. %, Hf – 15 wt. %. The cathode was sintered in the spark plasma sintering device SPS 25-10. The coatings were deposited on the "Nika" setup by vacuum-arc deposition from two sources. The first source is a cathode made of four-component Ti-Zr-Nb-Hf alloy (HES). The second cathode is made of molybdenum. A continuous rotation of the fixed samples was carried out with a speed of 8.0 rpm in the formation of coatings. The deposition parameters are given in Table 1.

The elemental composition of the coatings was studied using electron-ion scanning microscope Quanta 200 3D; the surface topography was investigated on Nowa NanoSEM 450. The structural stress state was studied on Rigaku Ultima IV and Rigaku Smart LAB diffractometers in Cu-K_α radiation (wavelength $\lambda = 0.154$ nm). To determine the adhesion strength, scratch resistance, a Revetest scratch tester (CSM Instruments) was used. The microhardness of the coatings was measured on an automated hardness tester AFFRI DM-8 by the micro-Vickers method. The tribotechnical tests of the coatings were performed by the standard "ball-disk" scheme on an automated high-temperature tribometer High-Temperature Tribometer (CSM Instruments) with fractographic analysis of the wear groove of the coatings and the wear scars on the counterbody (corundum ball with a diameter of 6 mm). The wear resistance tests were conducted in air at a load of 6 N, a linear velocity of 15 cm/s, a radius of wear curvature of 5 mm, and a stopping distance of 1200 meters. The groove depths were measured in 4 diametrically and orthogonally opposite sample regions using an automated precision contact profilometer Surtronic 25; and the mean values of the cross-sectional area and depth of the wear groove were determined.

Table 1 – Physical and technological deposition parameters

Series number	Coating	I_d, A	U_b, V	P_N, torr
1	(TiZrNbHf)N/MoN	140/100	40	3×10^{-3}
2	(TiZrNbHf)N/MoN	200/150	90	4×10^{-3}
3	(TiZrNbHf)N/MoN	150/100	150	3×10^{-3}

3. RESULTS AND DISCUSSION

The study of the growth morphology of multilayer coatings showed their sufficiently high uniformity and planarity for all technological deposition parameters. The drop non-uniformity was detected on the surface that did not lead to a significant distortion of planarity and average thickness (see Fig. 1b). The layer thickness was approximately equal to 50 nm.

The results of energy dispersive X-ray microanalysis (EDX method) showed that the molybdenum concentration in the coatings decreases significantly with increasing bias potential: from 32.06 wt. % at a bias potential of $U_b = -40$ V to the value of 15.23 wt. % at a bias potential of $U_b = -90$ V. In the future, the molybdenum concentration increases to 25.34 wt. % with increasing bias potential to $U_b = -150$ V (see Table 2).

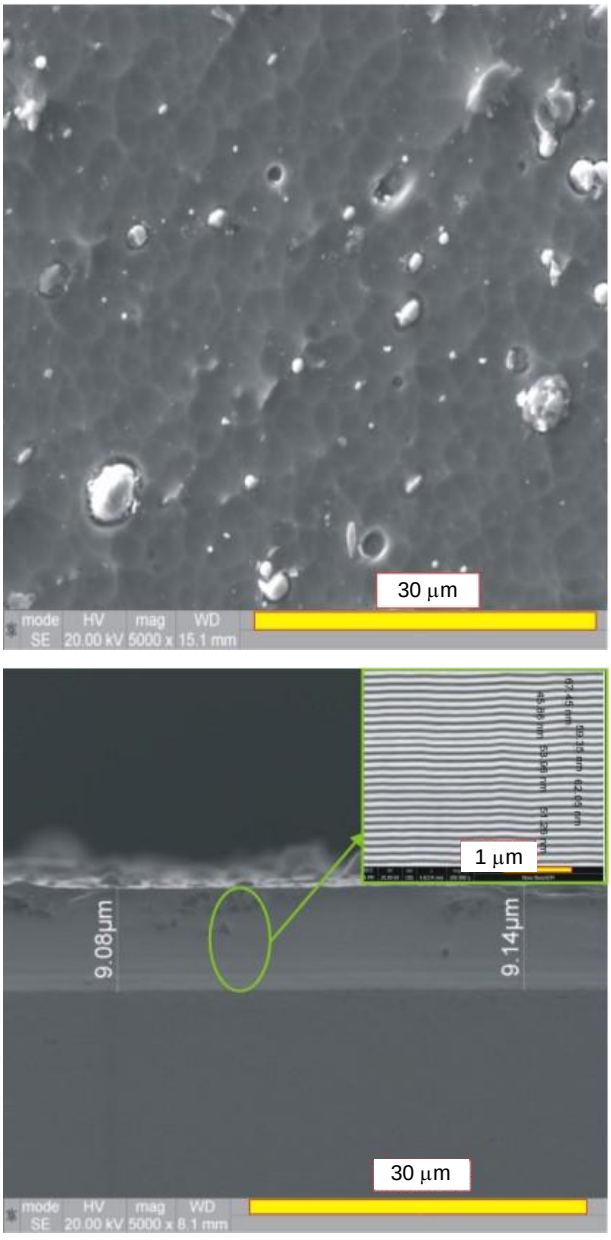

Fig. 1 – Image of the (TiZrNbHf)N/MoN system coating obtained at $P_N = 3 \times 10^{-3}$ torr, $U_b = -90$ V (series 2): a – surface topography and b – lateral cross-section of the multilayer coating on the substrate

An increase in the negative bias potential (U_b) leads to depletion of the coating of light atoms. The main reason for this is selective sputtering of light atoms during deposition from the growth surface.

The results of X-ray phase analysis indicate that the formation of phases with the cubic (fcc) crystal lattice is typical for all deposition modes both in layers based on a high entropy alloy and in layers based on molybdenum. In layers based on a high entropy alloy, this is a disordered solid solution (TiZrNbHf)N with the crystal lattice of the NaCl structural type; in the Mo-N system layers, this is γ-Mo_2N with the same type of the NaCl crystal lattice, but with a smaller lattice constant, as manifested in the shift of the diffraction peaks towards larger angles (see Fig. 2). In this case, the similarity of structural states in the layers based on a high entropy alloy and transition-metal nitrides, in particular MoN (a close ratio of the formed preferred orientations of crystallites in the layers), implies the interrelation between the structure of the layers during their growth. For coatings of the (TiZrNbHf)N/MoN system, the ratio between the atomic content of Mo and the metals of the second (TiZrNbHf) layer is almost not observed with increasing U_b, remaining in absolute value at the level of 51-53 wt. %.

The influence of the bias potential and the pressure of the working nitrogen atmosphere have a decisive effect on the phase composition and structural state of the coatings.

The supply of high negative potential $U_b = -150$ V leads to an increase in the degree of "chaotization" of the structure (the texture typical for small U_b does not appear for large U_b) and also to an increase in the dispersion of crystalline formations in the coating layers that is most pronounced for the γ-Mo_2N layers, in which the average crystallite size decreases from 54 nm to 37 nm with increasing U_b. This may be related to the additional generation of light diffusion paths when forming in the border area a solid solution of HES and Mo atoms as a result of radiation-stimulated mixing.

The annealing of the coatings in vacuum at a temperature of 973 K leads to a significant change in the content of nitrogen, titanium and impurity oxygen atoms in the coating obtained at high bias potential (Table 3).

The results of measuring the hardness of the coatings of the (TiZrNbHf)N/MoN system are shown in Fig. 3.

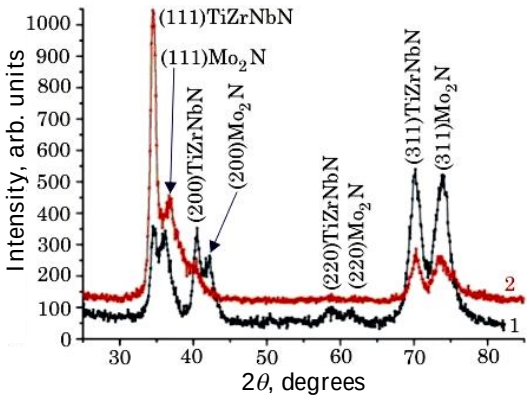

Fig. 2 – Regions of the X-ray diffraction spectra of the samples with the coating of the (TiZrNbHf)N/MoN system obtained at $P_N = 3 \times 10^{-3}$ torr: 1) $U_b = -40$ V (series 1) and 2) $U_b = -90$ V (series 2)

Table 2 – Elemental composition of the (TiZrNbHf)N/MoN coatings

Coating	Series	U_b, V	Elemental composition, wt. %					
			N	Mo	Ti	Zr	Hf	Nb
(TiZrNbHf)N/MoN	1	– 40	17.37	32.08	24.26	12.81	2.23	11.25
	2	– 90	20.64	15.23	25.46	32.54	0.93	5.20
	3	– 150	21.05	25.34	23.03	14.42	2.51	13.65

Table 3 – Elemental composition of the (TiZrNbHf)N/MoN coatings after annealing

Coating	Series	U_b, V	Elemental composition, wt. %						
			N	Mo	O	Ti	Zr	Hf	Nb
(TiZrNbHf)N/MoN	1	– 40	12.63	11.54	5.63	24.46	12.47	2.15	11.54
	2	– 90	16.33	25.76	3.84	23.29	14.65	2.47	13.67
	3	– 150	20.55	19.13	4.08	38.03	8.67	1.36	8.18

Table 4 – Tribological characteristics of the multilayer (TiZrNbHf)N/MoN system coating in the "ball-disk" tests

Series	Friction coefficient	Wear rate, $mm^3 \times N^{-1} \times mm^{-1}$		Remarks
		Counterbody	Coated samples	Counterbody material
1	0.74	8.7×10^{-7}	2.78×10^{-6}	Al_2O_3
2	0,83	2.24×10^{-6}	3.9×10^{-6}	Al_2O_3
2	0.57	2.59×10^{-4}	2.12×10^{-5}	Ac100Cr6 steel

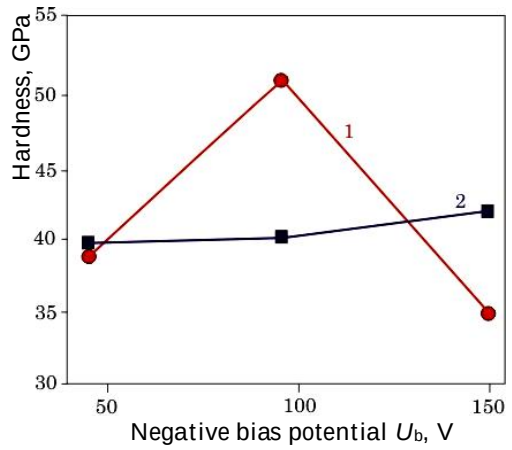

Fig. 3 – Change in the hardness of the (TiZrNbHf)N/MoN coatings obtained at $U_b = -90$ V, $P_N = 3 \times 10^{-3}$ torr: 1 – before annealing; 2 – after annealing

According to the measurement data shown in Fig. 3, the coatings deposited at a relatively low bias potential and a high concentration of zirconium, titanium and nitrogen exhibit the greatest hardness. This is due to the fact that metal mononitrides in the equilibrium state are characterized by the ability to form phases with the non-cubic crystal lattice that, seemingly, creates an additional barrier to the movement of dislocations at the interphase with nitrides possessing the HES cubic lattice and, thus, strengthens the material.

The reason for the decrease in hardness with increasing bias potential up to $U_b = 150$ V is the enhancement of mixing in the border area, which in thin layers (about 40-50 nm) leads to a high fraction of the mixed area in the solid solution state and, thereby, reduced hardness (see curve 1 in Fig. 3).

Annealing of the coatings in vacuum at 973 K obtained at a high bias potential ($U_b = -150$ V) not only does not decrease the coating hardness, but the hardness increases from 35 GPa to 42 GPa due to the ordering at elevated temperatures in high entropy nitride layers [9].

The results of the scratch tests show that the greatest pressure before destruction is inherent to the coatings obtained at a low value of $U_b = -90$ V and reaches the value of $L_{C5} = 124.9$ N (Fig. 4).

Samples of series 1 and 2 of (TiZrNbHf)N/MoN deposited at different values of the bias potential $U_b = -40$ V and $U_b = -90$ V are chosen as the samples for tribological tests. The photographs of friction tracks and the counterbodies obtained using scanning electronic microscopy are illustrated in Fig. 5. The results of tribotechnical tests are given in Table 4.

Visually, the friction tracks (see Fig. 5a) are characterized by the absence of barbs, chips and radial flaws that indicates high quality and adhesion strength of the coating. The average width of the friction track in the case of the counterbody of Al_2O_3 is equal to 654.88 μm (see Fig. 5b), and in the case of the counterbody made of the Ac100Cr6 steel, the track is various in thickness and has a non-uniform wear.

The reason for this non-uniform behavior is the adhesion of a relatively soft and ductile metal of the counterbody to the coating that increases the actual contact area and, in the future, the friction occurs, in fact, in a worn metal – counterbody pair. This fact is associated with a reduction of the fixed friction coefficient and an increase, thereby, in the steel ball wear.

A uniform abrasive wear of the rubbing pair with the removal of wear products and their accumulation along the groove edges was observed in the friction with the counterbody of Al_2O_3 (see Fig. 5a).

According to the results presented in [12], the amount of transferred material depends on the adhesive bond strength, which, in turn, depends on the electronic structure of the Al_2O_3-based counterbody and a multilayer coating and determines the possibility of forming solid solutions or intermetallic compounds with each other, as well as oxides stable at high temperatures. The above mentioned is associated with high values of the friction coefficient (see samples of the series 2) in tests with the counterbody of Al_2O_3 coatings, which include the high entropy (TiZrHfVNbTa)N nitride [13].

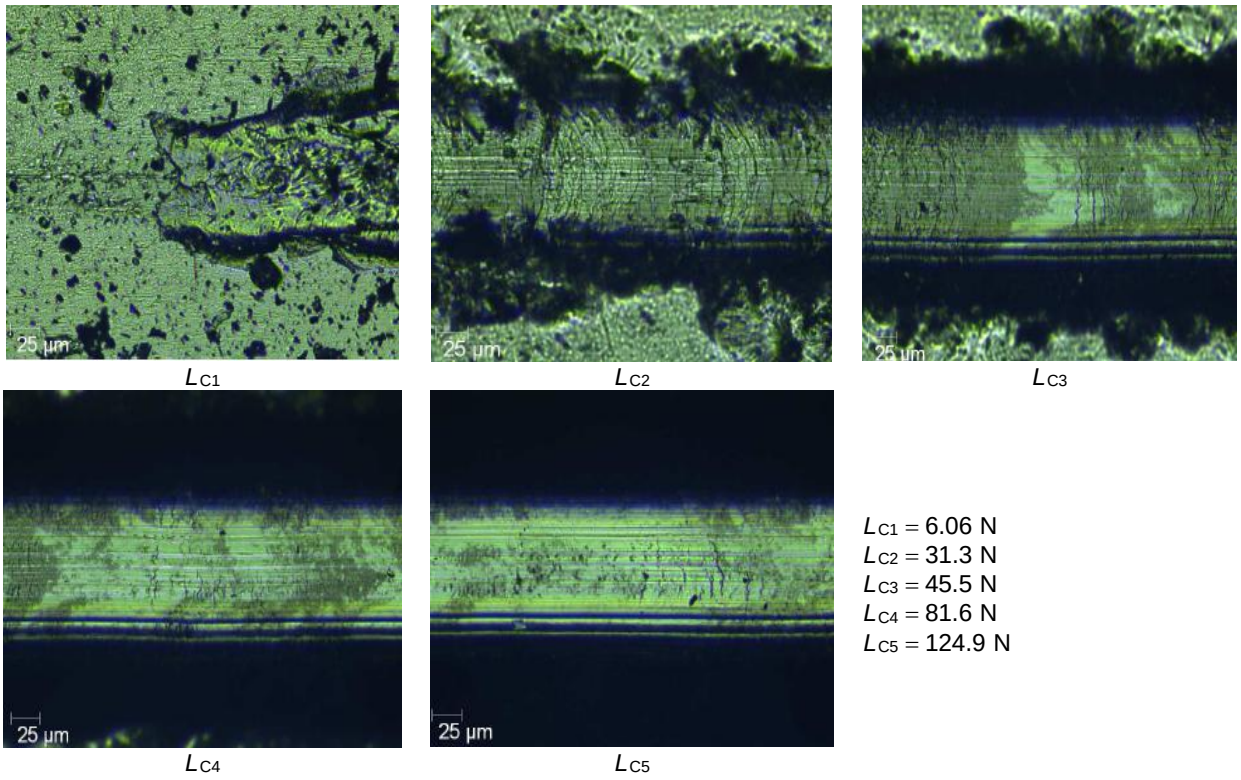

Fig. 4 – Images of the wear tracks and values of the critical loads for the (TiZrNbHf)N/MoN system coatings ($P_N = 3 \times 10^{-3}$ torr, $U_b = -90$ V)

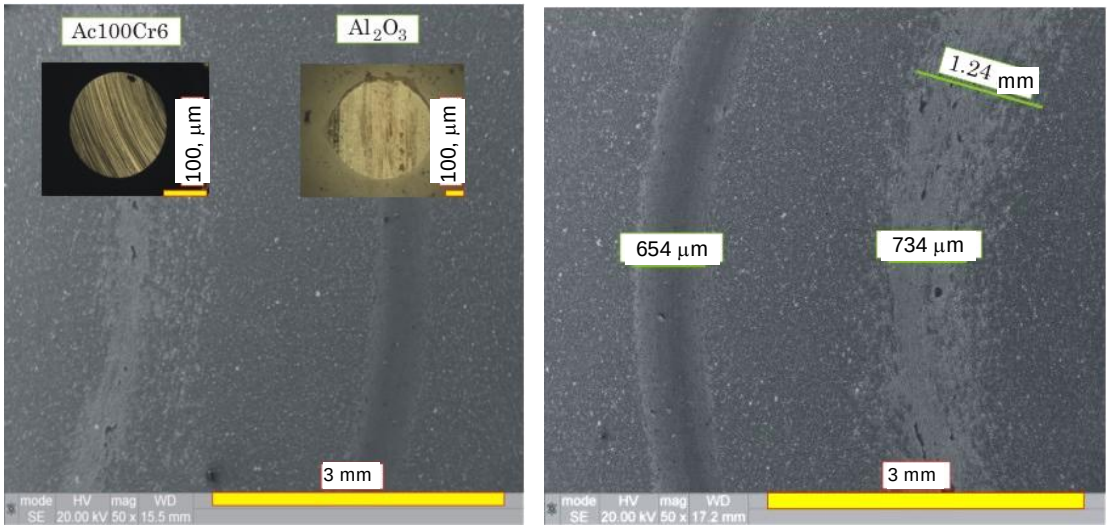

Fig. 5 – Images of the friction tracks in the "ball-disk" tests with the counterbody in the form of a ball of Al_2O_3 and Ac100Cr6 steel of a multilayer coating of the (TiZrNbHf)N/MoN system: a – with the detailing of the friction tracks by the counterbody type and b – with certain average sizes of the friction tracks for the counterbodies of two types

The coatings of the (TiZrNbHf)N/MoN system possess good wear resistance: the values of the wear for both types of the counterbody are in the range of (0.39-2.12) $\times$ $\times 10^{-5}$ mm$^3 \times$ N$^{-1} \times$ mm^{-1}. For the counterbody produced from artificial corundum Al_2O_3, the fixed wear is not high and is equal to 2.24×10^{-6} mm$^3 \times$ N$^{-1} \times$ mm^{-1} (see Table 4). For the counterbody made of Ac100Cr6 steel (the analogue of ShKh15), the wear increases by two orders of magnitude and amounts to the value of 2.59×10^{-4} mm$^3 \times$ N$^{-1} \times$ mm^{-1}.

Thus, a sufficiently high resistance of the multilayer (TiZrNbHf)N/MoN system coatings based on high entropy alloy nitrides to the counterbodies different in hardness and viscocity opens good prospects for using such coatings as protective ones under complex influences in the abrasive wear conditions.

The coatings are promising as protective ones for friction of machine parts and for protecting working surfaces of cutting tools operating under conditions of high cutting speeds of hard and superhard materials.

4. CONCLUSIONS

1. The surface morphology of the multilayer coatings of the (TiZrNbHf)N/MoN system is characterized by a sufficiently high uniformity and planarity for all technological deposition parameters.

2. It is shown that the formation of phases with the fcc cubic crystal lattice in both layers of the multilayer coatings is typical for all deposition modes of the multilayer (TiZrNbHf)N/MoN system coatings.

3. The multilayer (TiZrNbHf)N/MoN system coatings reach the highest hardness of 52 GPa for the deposition parameters of $U_b = -90$ V and $P_N = 3 \times 10^{-3}$ torr.

4. The results of the scratch tests show that the greatest pressure of $L_{C5} = 124.9$ N before destruction is inherent to the (TiZrNbHf)N/MoN system coatings obtained at a value of $U_b = -90$ V.

5. Annealing of the multilayer coatings in vacuum at 973 K obtained for high bias potential ($U_b = 150$ V) increases the coating hardness due to the ordering at elevated temperatures in high entropy nitride layers.

6. The multilayer (TiZrNbHf)N/MoN coatings have high wear resistance The wear values when using different counterbody types (Al_2O_3 and Ac100Cr6 steel) are in the range of (0.39-2.12) $\times 10^{-5}$ mm$^3 \times$ N$^{-1} \times$ mm^{-1}.

ACKNOWLEDGEMENTS

This work has been performed with the support of the Department of Internal and Personnel Policy of the Belgorod Region (Grant No. 11-GR, April 13, 2016) and with partial financial support of the Ministry of Education and Science of Ukraine (Grant No 0115U000477, 0115U003165 and 0115U003166).

REFERENCES

1. X. Chu, M.S. Wong, W.D. Sproul, S.L. Rohde, S.A. Barnett, *J. Vac. Sci. Technol.* A10, 1604 (1992).
2. S.F. Chen, Y.Ch. Kuo, Ch.J. Wang, S.H. Huang, J.W. Lee, Y.Ch. Chan, H.W. Chen, J.G. Duh, T.E. Hsieh, *Surf. Coat. Technol.* 231, 247 (2013).
3. O.V. Sobol', A.A. Andreev, S.N. Grigoriev, V.F. Gorban', M.A. Volosova, S.N. Aleshin, S.V. Stolbovoy, *Problem. Atomic Sci. Technol.* 4(74), 174 (2011).
4. A.D. Pogrebnyak, O.V. Sobol', V.M. Beresnev, P.V. Turbin, S.N. Dub, G.V. Kirik, A.E. Dmitrenko, *Tech. Phys. Lett.*+ 35 No 10, 925 (2009).
5. U.S. Nyemchenko, V.Ju. Novikov, O.V. Sobol', S.S. Grankin, E.M. Tulibiyev, A. Radko, *J. Nano- Electron. Phys.* 7 No 1, 01041 (2015).
6. U.S. Nyemchenko, V.M. Beresnev, O.V. Sobol, S.V. Lytovchenko, V.A. Stolbovoy, V.Ju. Novikov, A.A. Meylekhov, A.A. Postelnyk, M.G. Kovaleva, *Problem. Atomic Sci. Technol.* 1(101), 112 (2016).
7. A.D. Pogrebnjak, A.A. Bagdasaryan, I.V. Yakushchenko, V.M. Beresnev, *Russ. Chem. Rev.* 83 No 11, 1027 (2014).
8. U.S. Nyemchenko, V.Ju. Novikov, V.A. Stolbovoy, V.M. Beresnev, O.V. Sobol, *Problem. Atomic Sci. Technol.* 2(96), 139 (2015).
9. N.A. Azarenkov, O.V. Sobol, V.M. Beresnev, A.D. Pogrebnyak, D.A. Kolesnikov, P.V. Turbin, I.N. Toryanik, *Metallofiz. Nov. Tekhnol.* 35 No 8, 1061 (2013).
10. S.A. Firstov, V.F. Gorban, N.A. Krapivka, E.P. Pechkovsky, *Compos. Nanostructur.* 2, 5 (2011).
11. Y. Zhang, T.T. Zuo, Z. Tang, M.C. Gao, K.A. Dahmen, P.K. Liaw, Z.P. Lu, *Prog. Mater. Sci.* 61, 1 (2014).
12. N.K. Myshkin, M.I. Petrokovets, *Treniye, smazka, iznos. Fizicheskiye osnovy i tekhnicheskiye prilozheniya tribologii*, 368 (M: FIZMATLIT: 2007).
13. S.N. Grigoriev, O.V. Sobol, V.M. Beresnev, *J. Friction Wear* 35 No 5, 359 (2014).